Atmospheric air pressure plasma treatment of lignocellulosic fibres: impact on mechanical properties and adhesion to cellulose acetate butyrate

Alexis Baltazar-Y-Jimenez, Martina Bistritz, Eckhard Schulz, Alexander Bismarck

Accepted Manuscript

Atmospheric air pressure plasma treatment of lignocellulosic fibres: impact on mechanical properties and adhesion to cellulose acetate butyrate

Alexis Baltazar-y-Jimenez, Martina Bistritz, Eckhard Schulz, Alexander Bismarck

PII: S0266-3538(07)00204-7
DOI: 10.1016/j.compscitech.2007.04.028
Reference: CSTE 3705

To appear in: *Composites Science and Technology*

Received Date: 1 February 2007
Revised Date: 24 April 2007
Accepted Date: 30 April 2007

Please cite this article as: Baltazar-y-Jimenez, A., Bistritz, M., Schulz, E., Bismarck, A., Atmospheric air pressure plasma treatment of lignocellulosic fibres: impact on mechanical properties and adhesion to cellulose acetate butyrate, *Composites Science and Technology* (2007), doi: 10.1016/j.compscitech.2007.04.028

Atmospheric air pressure plasma treatment of lignocellulosic fibres: impact on mechanical properties and adhesion to cellulose acetate butyrate

Alexis Baltazar-y-Jimenez[1], Martina Bistritz[2], Eckhard Schulz[2] and Alexander Bismarck[1]*

[1] Department of Chemical Engineering
Polymer & Composite Engineering (PaCE) Group
Imperial College London
South Kensington Campus
London, SW7 2AZ, UK

[2] Bundesanstalt für Materialforschung und Materialprüfung (BAM), Laboratorium Vi.2.1,
Unter den Eichen 87, D-12205 Berlin, Germany
*Author for correspondence E-mail: a.bismarck@imperial.ac.uk;
Telephone: +44 (0) 2075945578; Fax. +44 (0) 2075945638

ABSTRACT

We report on the effect of atmospheric air pressure plasma (AAPP) treatment on the mechanical properties and interfacial behaviour of different lignocellulosic fibres to cellulose-acetate-butyrate (CAB), as an example for a renewable polymer. The impact of the AAPP treatment on the properties of abaca, flax, hemp and sisal fibres was studied by scanning electron microscopy and single fibre tensile tests. Single fibre pull-out tests were performed in order to determine the effect of AAPP on the apparent interfacial shear strength (τ_{IFSS}) of the (modified) fibres to CAB. After AAPP treatment, the tensile strength, Young's modulus and elongation at break of the lignocellulosic fibres reduced drastically and deteriorated further with extended treatment. The heat generated during the plasma treatment causes dehydratation of the fibres and the etching effect of plasma degrades their macrofibril structure. A goodness-of-fit analysis shows that the tensile strength of the pre- and post-treated fibres approximate a normal distribution. The interfacial shear strength (IFSS) increases for flax, hemp and sisal fibres after 1 min AAPP treatment, but decreases with prolonged treatment time for abaca and sisal fibres. The increase in τ_{IFSS} after short AAPP treatment (1 min) is due to the introduction of functional groups, cleaning of contaminant substances that hinder the adhesive process and enhanced surface roughness, which favours mechanical interlocking between the fibres and the matrix. Extended AAPP treatment seems to have induced weak boundary layers on the surface of the fibres, which reduced the IFSS to CAB.

Keywords: Agro-fibres, Fibre/Matrix Bond, Interfacial Strength.

Abbreviations: AAPP: Atmospheric Air Pressure Plasma. IFSS: Interfacial Shear Strength. CAB: Cellulose-Acetate-Butyrate.

1.0 INTRODUCTION

A number of surface modification methods have been used on lignocellulosic fibres in the past in order to remove the organic compounds attached to the hydrophilic surfaces of plant cell walls. These substances form a natural protective layer, but partially hinder the industrial exploitation of lignocellulosic fibres, especially in processes where the wettability behaviour, dyeability and adhesive properties of plant fibres have to be improved. Two broad kinds of surface modification treatments are available including physical (e.g. plasma and corona treatment) and chemical (e.g. mercerization, acetylation, coupling agents, polymer grafting, etc.), which introduce chemical bonding to the matrix in order to produce a highly cross-linked interphase [1]. Traditional surface modification methods have the disadvantage of producing a considerable amount of hazardous substances and vapours, which could pollute the environment and have to be disposed of appropriately.

A more environmentally friendly alternative is the use of plasma technologies. Plasma is a ionized gas containing a mixture of ions, electrons, neutral and excited molecules and photons [2]. During atmospheric air pressure plasma (AAPP) treatment, a high frequency electric current excites a feeding gas usually compressed air, into relatively low temperature plasma. Depending on the type and nature of the feed gases used, a variety of surface modifications can be achieved, including an increase or decrease of the surface energy, surface crosslinking and the introduction of reactive free groups [1]. The plasma treatment duration, magnitude of power, distance from the plasma nozzle to the substrate have been shown to be extremely important for the optimisation of interfacial shear strength (IFSS) and the eventual composite properties as suggested by Yuan et al. [3, 4].

It is generally agreed that some of the advantages of AAPP are the absence of polluting organic solvents required for its use, lack of hazardous waste, low operating costs, short treatment times and greater flexibility since it does not require of a vacuum-chamber [5].

The aim of the present work is to investigate the effect of atmospheric air pressure plasma on the mechanical properties of lignocellulosic fibres and its impact on interfacial adhesion behaviour of these fibres to CAB.

2.0 EXPERIMENTAL

2.1. Materials

Only lignocellulosic technical grade fibre bundles were investigated. Abaca fibres (Musa textilis Nee) were kindly supplied by Heritage Arts & Crafts (Kalibo, Aklan, the Philippines). These fibres are extracted by hand pulling, washed and sun-dried for one day (Legaspi, 2005, 2006, Heritage Arts & Crafts, personal communication). Belgian dew-retted flax fibres (Linum usitatissimum) were separated through a breaking-scutching-hackling process and kindly supplied by Wigglesworth & Co. (London, UK). Sisal (Agave sisalana) fibres were obtained from a local market in San Luis Potosi, Mexico. Sisal fibres were obtained through dew retting (or field retting), in which the sisal fibres are left in the field for 3-4 weeks until they are partially rotten through the combined action of temperature, bacteria and fungi in order to remove the cellulose fibres from the cementing substances, mainly hemicelluloses, lignin and pectin [6]. Sisal fibres are separated by placing them in a rudimentary tool made of wood where the fibres are pulled out by hand, washed and sun-dried for one day. Decorticated hemp fibres (Cannabis sativa) were kindly provided by Hemcore Ltd. (Bishops Stortford, Hertfordshire, UK). During the decortication process, the hemp fibres and the wooden stems are disaggregated using automated paired breaking rollers and carding systems (Hobson, 2004, 2006. Hemcore Ltd., personal communication), the fibres provided were mainly 10 mm in length mixed with some bark fibre.

Powdered cellulose-acetate-butyrate (CAB 500-5) (with approx. tensile strength 31 MPa, Young's modulus 0.3 GPa, elongation to break 130 %) was supplied by Eggar & Co. (Chemicals) Ltd., UK. Before any measurement, the lignocellulosic fibres were rinsed with distilled water for 10 min to remove water-soluble matter and subsequently vacuum-dried for 48 hrs at 70ºC.

2.2 Atmospheric Air Pressure Plasma Treatment

An Openair^{TM} plasma system (Plasmatreat GmbH, Steinhagen, Germany) was used to functionalise the surfaces of lignocellulosic fibres. The AAPP treatment was carried out at maximum power (10 kW) for duration of 1 min and 3 min. A small amount of technical fibres (3 g) were fixed longitudinally inside an inverted glass T-piece. The middle inlet was positioned under the plasma nozzle in an attempt to

confine the active plasma species around the fibres for the duration of the treatment (Fig. 1). The substrate was fixed at 30 mm from the plasma nozzle in order to avoid the thermal degradation of the lignocellulosic fibres.

The extent of the treatment time and distance from the plasma nozzle to the substrate had to be limited because of the thermally induced changes that could be seen directly after treatment; i.e. the fibres changed colour or even carbonised at closer ranges, whereas distances fixed at 50 mm and 70 mm were ineffective. Treatment time of 1 min, 3 min, 15 min and 25 min were investigated at fixed distances of 30 mm, 50 mm and 70 mm. However, it was found that treatment times in excess of 3 min produce a significant loss in the mechanical properties of the lignocellulosic fibres, thus rendering longer treatments unattractive, shorter treatment times of 15 s and 30 s were also ineffective. After treatment, the mechanical properties and adhesion behaviour of the fibres to CAB was measured.

2.3 Mechanical Properties

An Instron universal materials tensing machine model 4500 (Instron Ltd, High Wycombe, UK) was used to determine the mechanical properties of the lignocellulosic fibres conforming to the industrial standard test method ASTM D 3822-01 at an extension rate of 0.10 mm/min. At least twenty tests were performed for each gauge length used, i.e. 5 mm, 10 mm, 20 mm and 50 mm. Single fibres were glued onto cardboard tabs with cyanoacrylate adhesive and let to cure for 48 h. The specimens were brought to moisture equilibrium 72 h before the experiment inside a desiccator. The Young's modulus, tensile stress and elongation to break were calculated from the stress-strain curve obtained from the measurement, whereas the cross-sectional area of each fibre tested was determined from SEM micrographs.

Goodness- of-Fit

Statistically speaking, we were interested in determining if the tensile strength of the lignocellulosic fibres followed a normal distribution prior to and after AAPP treatment at the four different gauge lengths tested. For this reason a goodness-of-fit test was applied. The Shapiro–Wilk normality test is a method to gather evidence if a series of values approximates a normal distribution. This test requires defining two mutually excluding hypothesis, as to determine whether the data analysed approximates a normal distribution (i.e. null hypothesis, H_o) or not (i.e. alternative

hypothesis, H_i). The calculations were performed using the software Origin Pro v.7 at a significance level (α) of 0.05. The test computes a W-statistic, and a P-value, which measures the degree of plausibility of the hypothesis of the data, from which a decision can be drawn by comparison with the significance level. In other words, if the calculated P-value > 0.05 the null hypothesis (H_o) is true, it can be inferred that the data approximate a normal distribution. Whereas, a P-value < 0.05 rejects the null hypothesis, meaning that the data do not follow a normal distribution. More details on this statistical tool can be found in [7].

2.4 Adhesive Properties

Single Fibre Pull-Out Test

The samples used for the pull-out tests were embedded into a half-drop of molten polymer over a metal block using an embedding device that allows a perfect perpendicular orientation of the fibre to the matrix surface at a defined embedded length without bending the fibre. The method is further described in [8]. The tests were performed in a laboratory-made apparatus with a rigid frame at a constant speed of 0.20 μm/s. At least six runs were performed using single fibres with known cross-sectional area. Once the polymer drop cooled down and solidified the test was started and the load-displacement curve, as well as the embedded length used in each experiment was recorded. The apparent interfacial shear strength (τ_{IFSS}) was calculated from the maximum load (F_{max}) required to debond the fibre from the matrix, in conjunction to the fibre-embedded area (A_e) as shown in equation (1):

$$\tau_{IFSS} = \frac{F_{MAX}}{A_e} \quad (1)$$

where A_e is the embedded fibre area which was measured directly from SEM micrographs.

Critical Length

The critical fibre length (L_c) is a critical design parameter for composites because it provides essential information about the length at which the fibre achieves maximum load, thus transferring the stresses at the fibre-matrix interface. In the instance where the fibre length is smaller than the critical length, there is practically

no stress transfer and the fibre-matrix interface tends to fail. The critical fibre length was calculated using the approach of Kelly and Tyson [9] showed in equation (2):

$$L_c = \frac{\sigma_f A_f}{2\tau} \quad (2)$$

where σ_f is the fibre tensile strength, A_f the cross-sectional area of the fibre and τ is the apparent interfacial shear strength (IFSS) determined experimentally in the pull-out test.

2.5 Scanning Electron Microscopy

The surface morphology and cross-section of the untreated and AAPP-treated lignocellulosic fibres was examined using a scanning electron microscope JSM-5610 (Jeol Ltd, Herts, UK) with an initial accelerating voltage of 10 kV. The samples were gold sputtered (Emitech K550, Quorum Technologies Ltd, UK) for 3 min prior to examination to ensure good conductivity.

3.0 RESULTS AND DISCUSSION

Table 1-2 summarise the chemical composition and mechanical properties of the lignocellulosic fibres investigated. A simple hierarchical model in which the cellulose microfibrils are embedded in a matrix of hemicelluloses and lignin is usually used to explain the microstructure of many plant and wood fibres [10]. Hearle [11] improved the latter model by showing that the crystalline cellulose fibrils embedded in a non-crystalline matrix have a spiral arrangement that regulates the mechanics of extension of the fibrils, consequently deformation of the fibrils takes place either by stretching or by extension of the fibrils. The spiral arrangement of the crystalline cellulose regions form the microfibrillar angle, which regulates the stiffness of the macrofibrils and provide rigidity to the crop [12]. It is generally agreed that the major contributor to the overall properties of the fibre is the secondary wall (S2), in which a thicker matrix of hollocelluloses, hemicelluloses, lignin and pectins act as the matrix for the cellulose microfibrils [13]. Moreover, the chemical composition of the lignocellulosic fibres is associated to the conditions under which the plant was grown and the retting and separation method used to extract the fibres from the crop [14].

3.1 Chemical Composition of the Fibres

The experimental determination and chemical composition of the lignocellulosic fibres presented in this report was previously reported in Ref. [15] and it is summarised in Table 1. The main constituents of this kind of plant fibres are cellulose, hemicelluloses and lignin, but also small amounts of different free sugars, hollocelluloses, starch and pectins, hemicelluloses, proteins, several mineral salts [12], and extractives such as waxes, fatty alcohols, fatty acids and different esters [16]. As it can be seen in Table 1, flax and hemp have the highest cellulose content, both with approx. 75 wt.-%, whereas abaca and sisal fibre have only (approx.) 64 wt.-%, and 48 wt.-%, respectively. Similar values of 71 wt.-% and 74 wt.-% were reported by [17] for flax and hemp, whereas [18] and [19] reported comparable values of 65 wt.-% and 47 wt.-% for abaca and sisal fibre, respectively. Abaca has the highest lignin content of approx. 15 wt.-%, and the inorganic content of all the fibres is in the range from 1.1 wt.-% to 4.5 wt.-%.

3.2 Mechanical Properties

Table 2 shows the average diameter and mechanical properties of the lignocellulosic fibres investigated. The data fit well into the range published [17, 20, 21]. During testing, the original and AAPP treated fibres failed in brittle manner, i.e. they exhibit a linear or Hookean region and then a sharp drop in strength after ultimate failure stress was exceeded (Fig. 2). All tested fibres have a similar tensile strength at most gauge lengths; the elongation at break reduces with increase gauge length and the Young's modulus increases with increasing gauge length. Untreated hemp fibres show a peak in the tensile strength and Young's modulus at 10 mm length because the decortication process used to extract hemp fibres produces fibres with a predominant length of approx. 10 mm, meaning that longer fibres are more likely to have internal and surface flaws, such as weak points, damaged areas and micro-compressions.

AAPP treated fibres show a drop in the tensile strength and elongation at break that can be partially linked to the introduction of defects (e.g. cracks and pits) onto the surface of the fibres after plasma, the longer the exposure to the plasma treatment the higher the flaw population. Therefore, larger gauge lengths on AAPP treated lignocellulosic fibres will have a larger flaw population and lower tensile strength and

elongation at break values. Additionally, the etching and thermal effect of plasma weakens and damages the macro- and microfibrils because the temperature reached during AAPP treatment ranged between 140˚C and 180˚C (measured by means of a thermocouple), which is near the temperature in which most lignocellulosic fibres start to suffer rapid changes in mass loss [22]. LeVan [23] suggested that the loss of mass and moisture of lignocellulosic fibres reduces its tensile properties at approx. 100˚C, whereas extended thermal exposition produces permanent changes in the fibre morphology, diameter, weight and odour. Cellulose and hemicelluloses start to break down in the temperature range of 180˚C to 250˚C, which has an effect on the tensile strength of the lignocellulosic fibres.

Theoretically, the higher cellulose content (approx. 64 wt.-%) and lower microfibrillar angle (11˚) [18] for abaca fibres should result in a higher tensile strength than the one for sisal, which has approx. 48 wt.-% cellulose content and 10˚-22˚ microfibrillar angle [17]; however, that was not observed (Table 2). The higher amount of lignin and hemicelluloses in abaca fibres (approx. > 30 wt.-%) forming amorphous regions in the microfibrils [12] allow the propagation of cracks among the interface of the fibrils and within the technical fibre more easily when exposed to mechanical stress, as it can be seen in Figs. 3-6 for a single abaca, flax, hemp and sisal fibre bundle before and after tensile testing, respectively.

After tensile testing, the cross-sectional area of the abaca, flax and hemp fibres displays multiple cracks (Figs. 3-5, pointed with arrows) because the stress induced during testing separated the individual fibrils making up the technical fibres, probably through weak regions possibly composed of amorphous lignin and hemicelluloses. In contrast, the cross-sectional area of the sisal fibre (Fig. 6) shows a minimum amount of cracks only at the top part of the fibre.

3.3 Shapiro-Wilk Normality Test

Table 3 summarises the W-statistic and P-value obtained from the Shapiro-Wilk normality test performed on the measured tensile strength data of all the lignocellulosic fibres prior- and after- AAPP treatment. Fig. 7 shows that the data for the untreated, 1 min and 3 min AAPP treated abaca fibre, which approximates a normal distribution. There are many different probability distributions that may be used to analyse data, among them the bimodal, gamma, normal and Weibull, etc.

However, many naturally occurring populations tend to approximate a normal distribution [24], whereas the Weibull distribution is often useful to analyse product failures in the field of life data analysis, reliability and maintenance applications or to predict the homogeneity of a material [25]. It is likely that the tensile strength of the lignocellulosic fibres approximates a normal distribution, especially because it is not clear if the weakest-link model is an accurate way to describe if lignocellulosic fibres produce sudden catastrophic failure due to the growth of surface located flaws and/or to bulk located flaws, or due to both, as suggested by Zafeiropoulos et al. [21]. Furthermore, Bennett et al. [26] suggested that the presence of flaws (at least in carbon fibres) is not the true cause of low fibre strength, but the relatively continuous presence of misoriented crystalline regions (and possibly amorphous regions in the case of lignocellulosic fibres) surrounding some of the flaws; consequently the suitability of a Weibull statistical analysis in the case of highly heterogeneous lignocellulosic fibres could be debatable. According to the goodness-of-fit test performed the data approximates a normal distribution. Each set of data (i.e. tensile strength of the untreated, 1 min and 3 min AAPP treated fibres) was analysed using the same the null hypothesis (H_0) and alternative hypothesis (H_1), expressed as:

H_0: data approximate a normal distribution.

H_i: data do not approximate a normal distribution.

If the P-value obtained in the normality test is less than α (P-value > 0.05) it can be inferred that the tensile strength population approximates a normal distribution. For a normally distributed population, it can be expected that 99.7% of the points of the population will lie in the interval given by [μ -3σ, μ + 3σ], and approx. only 0.3 % will fall outside, where μ is the mean average of the population, and σ the standard deviation [27].

3.4 Surface Morphology

Figs. 8-11 show the surface morphology of the lignocellulosic fibres investigated before and after 1 min and 3 min of AAPP treatment. It is generally agreed that the primary wall of the lignocellulosic fibres is formed with fats, fatty acids, fatty alcohols, phenols, terpenes, steroids, and waxes [12, 28] gives the surface of the untreated fibres (Figs. 8-11a) an heterogeneous appearance; whereas the

subsequent secondary layers form a complex matrix of hemicelluloses, hollocelluloses, lignin, pectins and proteins.

Figs. 8- 11 reveal changes in the surface morphology of all the lignocellulosic fibres after 1 min and 3 min of AAPP treatment, respectively. A roughed surface morphology and a large number of defects in the form of cracks, pits and corrugations that are produced after 1 min of AAPP treatment (Figs. 8-11b); these defects may be partially due to the etching effect of plasma and exposure to elevated temperature during plasma, which may make expand the flaws already present on the fibres. The deterioration of the surface morphology is more severe after 3 min of treatment as greater amount of cracks, pits and deeper corrugations are visible (Figs. 8-11c).

3.5 Adhesion Behaviour

Tables 4-5 and Figs. 12-16 show the results obtained from the single fibre pull-out tests between the lignocellulosic fibres to CAB. The apparent interfacial shear strength (τ_{IFSS}) is generally regarded as a measure of practical adhesion, as it provides essential information about the form in which stress transfers from reinforcing fibres to the matrix. It is possible to determine τ_{IFSS} between thermoplastic matrices and single lignocellulosic fibres using the pull-out technique as shown by [29].

Fig. 13 is a representative example of the force-displacement curves obtained by pulling out untreated and plasma treated fibres of similar embedded length (i.e. ≈ 0.25 mm) form a CAB matrix droplet. The shape of the curves point to a non-catastrophic failure of the interface because after reaching the maximum debonding force, the interface is still carrying part of the load, thus producing significant plastic deformation at the interface. This latter is most probable due to increased roughness/greater exposition of microfibrils after AAPP treatment, which interacts to a greater extent with the matrix, rather than with the macrofibril itself. SEM images of fibres pulled out from CAB (Fig. 14a) and the corresponding matrix droplets (Fig. 14 b,c) were taken to investigate the fracture behaviour. The SEM micrographs (two are exemplarily shown in Fig. 14 b,c) show that no wetting cone formed when sisal is brought in to contact with the CAB polymer melt. Three factors determine whether or not a wetting cone forms: i) the contact angle between fibre and polymer melt which is a function of the surface tensions of both materials, ii) the melt is flowing under

gravity and thus is moving relative to the fibre and iii) the polymer shrinks onto the fibre during the cooling process. During the pull-out of the embedded fibre, the weakest part of the model composite fails. Usually, the highest stresses arise in the region, where the fibre is in contact with the polymer. As can be seen from the SEM images of the droplets after pull-out the matrix (Fig. 14 b,c) seems to shrink tightly onto the fibre. It seems that the failure of the single fibre composite starts at the fibre/matrix interface inside the droplet. The fracture type is related to the fibre roughness; however, it is complicated by the fact that some of the fibres fail insight the droplet (Fig. 14c), which also explains the large scatter of the experimental data (Fig. 16). In these cases, no energy required to fracture the matrix to separate the meniscus from the droplet. Therefore, the fibres after being pulled-out of the matrix are clean (Fig. 14a).

Fig. 15 shows τ_{IFSS} as function of embedded fibre length L_e. The dependence of τ_{IFSS} on the embedded fibre length allows distinguishing from brittle and ductile fracture behaviour [39]. τ_{IFSS} decreases with increasing embedded fibre length indicating a brittle failure behaviour. To determine τ_{IFSS} the maximum pull-out force measured during the pull-out of a sisal fibre from CAB is plotted as function of the embedded fibre area (A_e) (Fig. 16). The τ_{IFSS} was determined by obtaining the slope of the linear fits for each treatment [40]. In order to obtain comparable indicative results the linear regression was forced through zero because no energy was required to fracture the matrix (see Figs. 14 a,b). Again, the relatively large scatter of the data is most likely due to the fact that the technical lignocellulose fibres partially and uncontrollably fail inside the matrix (Figs. 14 a,b). Nevertheless, a slight increase in τ_{IFSS} after 1 min AAPP treatment is observed. But prolonging the AAPP treatment time leads to a reduction in τ_{IFSS}. Yuan et al. [38] reported a slight increase in τ_{IFSS} from 2.5 MPa to 3.1 MPa with lower air-plasma treatment time on sisal fibres embedded into a polypropylene matrix only to decrease again to 1.4 MPa with extended treatment measured using the fibre pull-out technique.

Table 4 summarises the obtained data. A slight increase in τ_{IFSS} was observed after 1 min AAPP treatment with the exception of the abaca fibres, whereas prolonged treatment reduces τ_{IFSS} for sisal fibres and abaca[†]. Luo et al. [30] reported a similar

[†] It is unlikely that 3 min of AAPP treated flax and hemp fibres will have a significant improvement in τ_{IFSS}, for this reason they were not measured.

τ_{IFSS} value of 8.23 MPa for pineapple fibre embedded into a poly-hydroxybutyrate-co-valerate (PHBV) measured using a similar technique. The increase in τ_{IFSS} after plasma treatment is the result of the combined effect of: 1) the modification of the surface chemistry by the introduction of functional groups [31] (in the case of atmospheric air gas plasma treatment these groups are most probable carboxyl, peroxy, hydroperoxy, amine and nitroso [32]) onto the outer structure that promotes further interactions with the surrounding polymer matrix [33]; 2) removal of contaminant substances, especially non-cellulose compounds like waxes, and fatty oils that cover the surface of the lignocellulosic fibres [34] and hinder the adhesive process; and 3) etching of the surface treated may partially increase the contact area of the lignocellulosic fibres, exposing the microfibrils and roughening the surface (see Figs. 8-11 b,c), thus promoting interfacial bonding through interlocking. The reduction of τ_{IFSS} for abaca and sisal fibres (Table 4) after extended AAPP may be partially attributed to the formation of a "weak boundary layer" (WBL), which acts as a low cohesion barrier between the lignocellulosic fibre and CAB. Stehr et al. [35] suggested that mechanical fibre degradation, e.g. roughened surfaces and loosely attached fibrils (Fig. 8-11c), which may be produced during the exposition to the environment in the AAPP jet, lead to "mechanically weak boundary layers" (MWBL); in addition, the hydrophobic extractives present on lignocellulosic fibres, (such as fats, fatty acids, sterols and waxes, and hydrophilic extractives e.g. sugars, phenols, tannins and proteins) may migrate to the surface of the fibres producing weak adhesive bonds or "chemical weak boundary layers" (CWBL). Both, CWBL and MWBL, are weak boundary layers, i.e. a layer of lower mechanical strength than the bulk material which develops on the surface of the material and acts as a barrier with low adhesion between the substrate and the surrounding phase. However, it most probable that the reduction in interfacial shear strength of the aforementioned fibres is due to the formation of a mechanical weak boundary layer (MWBL) only. Other authors have also argued that damaged lignocellulosic fibres may lead to weaker adhesive bonds, including Bröker et al. [36] who pointed out to the loss in strength and damaged surfaces of wood fibres for the weak mechanical and chemical adhesion to an epoxy resin. Yuan et al. [37] who suggested that the extended treatment of sisal fibres with air plasma damaged their surface morphology decreasing τ_{IFSS} to a polypropylene matrix.

Table 5 shows the critical fibre length (L_c) and the data used to determine L_c. L_c may be defined as the minimum fibre length required allowing tensile failure of the fibre, rather than shear failure of the interface, i.e., the minimum fibre length needed for the stress to reach the fracture stress of the fibre. L_c is a function of the properties of the reinforcement and the fibre-matrix interface, thus, L_c varies considerably in the literature, for example, Yuan et al. [37] reported a L_c of approx. 8 mm for untreated sisal embedded in a polypropylene matrix. Ideally, the maximum tensile strength of the fibres can only be exploited if the fibres can be stressed until fracture without being pulled out (i.e. $L_e > L_c$). If $L_e > L_c$ the tensile stress in the fibre will reach the fracture stress and it would break. However, if $L_e < L_c$ the bond will be broken and the fibre extracted [40].

4.0 CONCLUSIONS

We reported on the effect of atmospheric air pressure plasma (AAPP) treatment on the mechanical properties and interfacial behaviour between various AAPP treated lignocellulosic fibres and cellulose acetate butyrate. The mechanical properties of technical fibres were determined by means of single fibre tensile tests at different gauge lengths. The impact of AAPP of natural fibres on the practical adhesion was studied by single fibre pull-out tests. AAPP treatment induces changes in the surface morphology of the lignocellulosic fibres, especially with extended treatment. The tensile strength, Young's modulus and elongation to break decreased significantly after 1 min and 3 min AAPP treatment, because of the heat and etching effect of the atmospheric air plasma, which weakens and damages the macro- and microfibrils of the lignocellulosic fibres due to loss of mass and moisture. The Shapiro-Wilk normality test was performed on the tensile test data allows to infer that the tensile strength of the pre- and post- treated fibres approximates a normal distribution.

The interfacial shear strength (τ_{IFSS}) increases only marginally for flax, hemp and sisal fibres after 1 min AAPP treatment, but decreases with prolonged treatment time for abaca and sisal fibres, probably due to the formation of weak boundary layers (WBL). The reduction in interfacial shear strength of the aforementioned fibres is most probably due to the formation of a mechanical weak boundary layer (MWBL)

only. As a general trend, the critical fibre length reduced for most fibres after 1 min AAPP treatment, with the exception of abaca fibres.

ACKNOWLEDGMENTS

A. Baltazar-y-Jimenez gratefully acknowledges the Mexican Council on Science and Technology (CONACYT) for providing his studentship. The authors are grateful to Wigglesworth & Co. (UK), Hemcore Ltd. (UK) and Heritage Arts & Crafts (the Philippines) for supplying the samples.

REFERENCES

[1] Bledzki AK, Reihmane S, Gassan J. Properties and modification methods for vegetable fibres for natural fibre composites. J Appl Polym Sci 1996;(59):1329-1336.

[2] Shenton MJ, Lovell-Hoare MC, Stevens GC. Adhesion enhancement of polymer surfaces by atmospheric plasma treatment. J Phys D: Appl Phys 2001;(34):2754-2760.

[3] Yuan X., Jayaraman K, Bhattacharyya D. Effects of plasma treatment in enhancing the performance of woodfibre-polypropylene composites. Composites A 2004;(35):1363-1374.

[4] Yuan X., Jayaraman K., Bhattacharyya D. Mechanical properties of plasma-treated sisal fibre-reinforced polypropylene composites. J Adhes Sci Technol 2004;(18):1027-1045.

[5] Shenton M.J., Stevens G.C. Surface modification of polymer surfaces: atmospheric plasma versus vacuum plasma treatments. J Phys D: Appl Phys 2001;(34):2761-2768.

[6] Dodd RB, Akin DE. Recent developments in retting and measurement of fibre quality in natural fibres: Pro and cons. In: Mohanty Ak, Mirsa M, Drzal Lt, Natural fibres, biopolymers and their composites, Boca Raton:CRC Press,2005.

[7] Shapiro SS, Wilk MB. An analysis of variance test for normality. Biometrika 1965;(3):591-611.

[8] Hampe A, Kalinka G, Meretz S, Schulz E. An advanced equipment for single-fibre pull-out test designed to monitor the fracture process. Composites 1995;(26):40-46.

[9] Kelly A, Tyson WR. Tensile properties of fibre-reinforced metals - copper/tungsten and copper/molybdenum. J Mech Phys Solids 1965;(13):329-350.

[10] Kerr AJ, Goring DAI. Ultrastructure arrangement of the wood cell wall. Cellulose Chem Techn 1975;(9):563-573.

[11] Hearle JWS. The fine structure of fibres and crystalline polymers (iii). Interpretation of the mechanical properties of fibres. J Appl Polym Sci 1963;(7):1207-1223.

[12] Rowell RM, Han JS, Rowell JS. Characterisation and factors effecting fibre properties. In: Frollini E, Leao Al, Mattoso Lhc, Natural polymers and agro-fibres bases composites, Sao Carlos - S.P., Brazil:Embrapa Instrumentação Agropecuária,2000.

[13] Nishino T. Natural fibre sources. In: Baillie C, Green composites: Polymer composites and the environment, Boca Raton:CRC Press,2004.

[14] Morrison III WH, Archibald DD, Sharma HS, Akin DE. Chemical and physical characterization of water- and dew-retted flax fibres. Ind Crops Prod 2000;(12):39 - 46.

[15] Baltazar-y-Jimenez A., Bismarck A. Wetting behaviour, moisture up-take and electrokinetic properties of lignocellulosic fibres. Cellulose 2007;(14):115-127.

[16] Ribitsch V, Stana-Kleinschek K, Jeler S. The influence of classical and enzymatic treatment on the surface charge of cellulose fibres. Colloid Polym Sci 1996;(274):388-394.

[17] Bismarck A, Mishra S, Lampke T. Plant fibres as reinforcement for green composites. In: Mohanty Ak, Mirsa M, Drzal LT, Natural fibres, biopolymers and their composites, Boca Raton:CRC Press,2005.

[18] Chand N, Tiwary RK, Rohatgi PK. Bibliography resource structure properties of natural cellulosic fibres: An annotated bibliography. J Mater Sci 2002;(23):381-387.

[19] Kozlowski R, Wladyka-Przybylak M. Uses of natural fibre reinforced plastics. In: Wallenberg F., Weston N., Natural fibres, plastics and composites, USA:Kluwer Academic Publishers,2004.

[20] Coutts RSP. Banana fibres as reinforcement for building products. Journal of Mater Sci Lett 2002;(9):1235-1236.

[21] Zafeiropoulos NE, Dijon GG, Baillie CA. A study of the effect of surface treatments on the tensile strength of flax fibres (i). Application of gaussian statistics. Composites A 2007;(38):621-628.

[22] Kumar S, Varma I. Degradation studies of polycaprolactone in banana fibres reinforced thermoplastics composites. J Marcromol Sci Phys 2006;(45):153-164.

[23] LeVan SL. Thermal degradation. In: Schniewind Ap, Concise Encyclopaedia of Wood & Wood-based Materials, New York:Pergamon Press,1989.

[24] Ross SM. Distributions of sampling statistics. In: Elsevier, Introductory Statistics. San Diego:Elsevier Academic Press,2005.

[25] Rowell R.M., Han J.S., Rowell J.S. Characterisation and factors effecting fibre properties. In: Frollini E, Leao Al, Mattoso Lhc, Natural polymers and agro-fibres bases composites, Sao Carlos - S.P., Brazil:Embrapa Instrumentação Agropecuária,2000.

[26] Bennett SC, Johnson DJ, Johnson W. Strength-structure relationships in pan-based carbon fibres. J Mater Sci 1983;(V18):3337-3347.

[27] Ross SM. Normal random variables. In: Elsevier, Introductory statistics., San Diego: Elsevier Academic Press,2005.

[28] Lee BG, Han JS, Rowell RM. Oil sorption by lignocellulosic fibres. In: Kenaf properties, processing and products, Mississippi State University:Ag & Bio Engineering,1999.

[29] Stamboulis A, Baillie C, Schulz E. Interfacial characterisation of flax fibre-thermoplastic polymer composites by the pull-out test. Angew Makromol Chem 1999;(272):117-120.

[30] Luo S, Netravali AN. Interfacial and mechanical properties of environment-friendly 'green' composites made from pineapple fibres and poly(hydroxybutyrate-co-valerate) resin. J Mater Sci 1999;(34):3709-3719.

[31] Bismarck A, Springer J. Influence of plasma treatments on the wettability of material surfaces. In: Hubbard A, Encyclopaedia of Surface and Colloid Science, 2nd Ed. New York:Marcel Dekker,2002.

[32] Baltazar-y-Jimenez A, Bismarck A. Surface modification of lignocellulosic fibres in atmospheric air pressure plasma. (submitted) 2007.

[33] Li R, Lin Y, Mai YW. Application of plasma technologies in fibre-reinforced polymer composites: A review of recent developments. Composites A 1997;(28):73-86.

[34] Khammatova VV. Effect of high-frequency capacitive discharge plasma on the structure and properties of flax and lavsan materials. Fibre Chem (Translation of Khimicheskie Volokna) 2005;(37):293-296.

[35] Stehr M, Johansson I. Weak boundary layers on wood surfaces. Journal of Adhes Sci Technol 2000;(14):1211-1224.

[36] Bröker FW, Korte K. Festigkeiten von hirnholzverbindungen mit dicken epoxidharzfugen. Holz Roh-Werkst. 1994;(52):287-292.

[37] Yuan X, Jayaraman K, Bhattacharyya D. Plasma treatment of sisal fibres and its effects on tensile strength and interfacial bonding. J Adhesion Sci Technol 2002;(16):703-728.

[38] Meretz S, Auersch W, Marotzke C, Schulz E, Hampe A. Investigation of morphology-dependent fracture behaviour with the single-fibre pull-out test. Composites Sci Technol 1993;(48):285-290.

[49] Subramanian RV, Jakubowski JJ, Williams FD. Interfacial aspects of polymer coating by electropolymerization. J Adhesion 1978;(9):185-195.

[40] Matthews FL, Rawlings RD. Fracture mechanisms and toughening mechanisms. In: F.L. Matthews, R.D. Rawlings, Composite materials: Engineering and science, Boca Raton:CRC Press,2000.

FIGURE

Figure 1

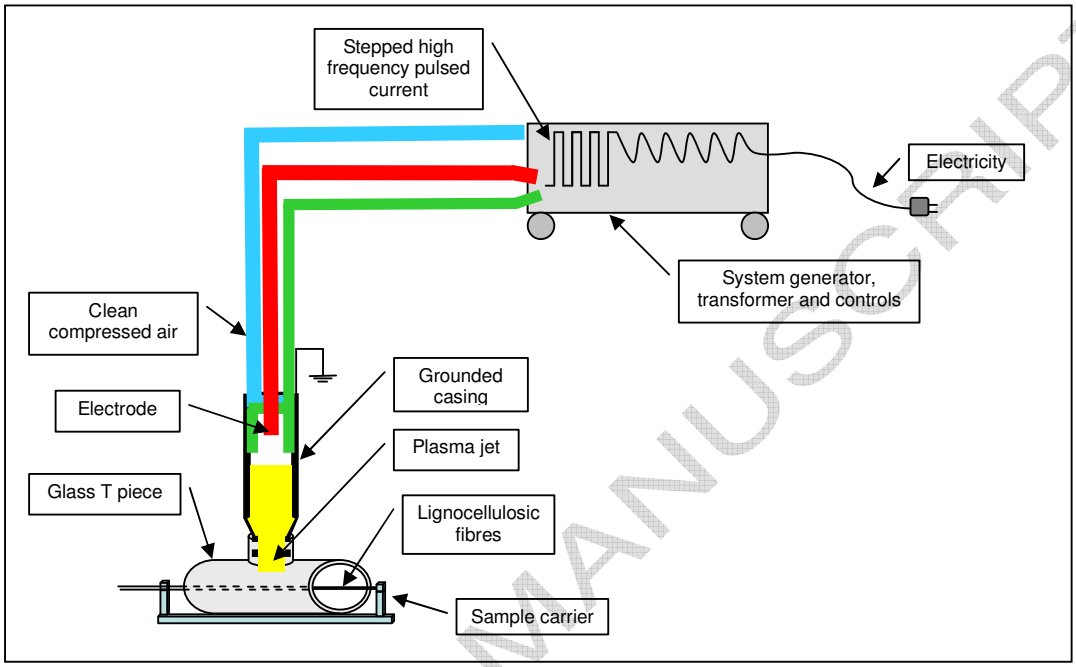

Figure 2

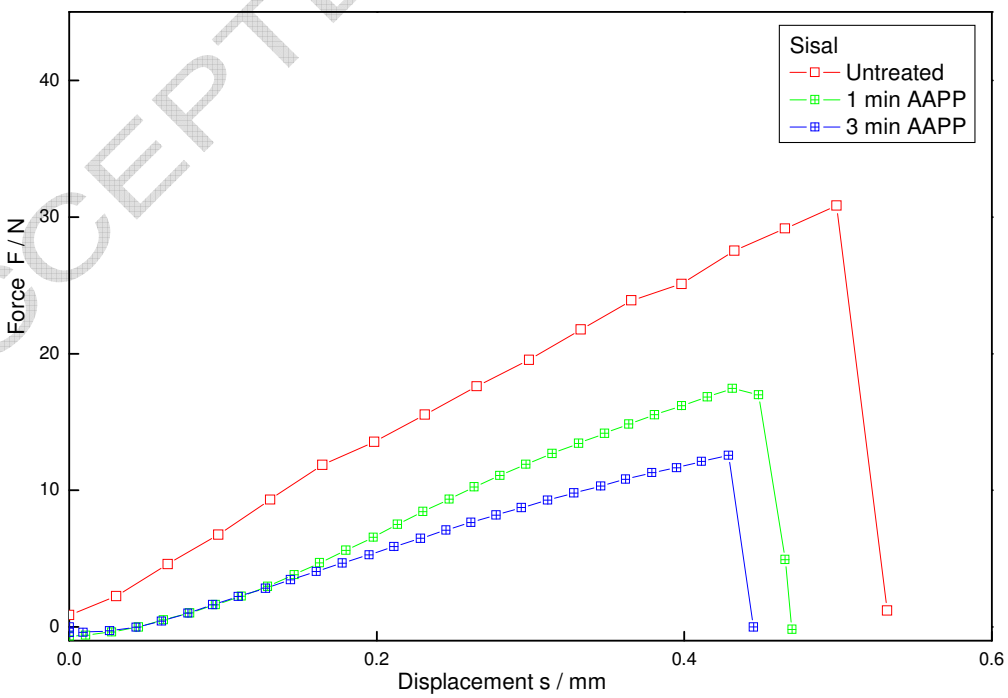

Figure 3

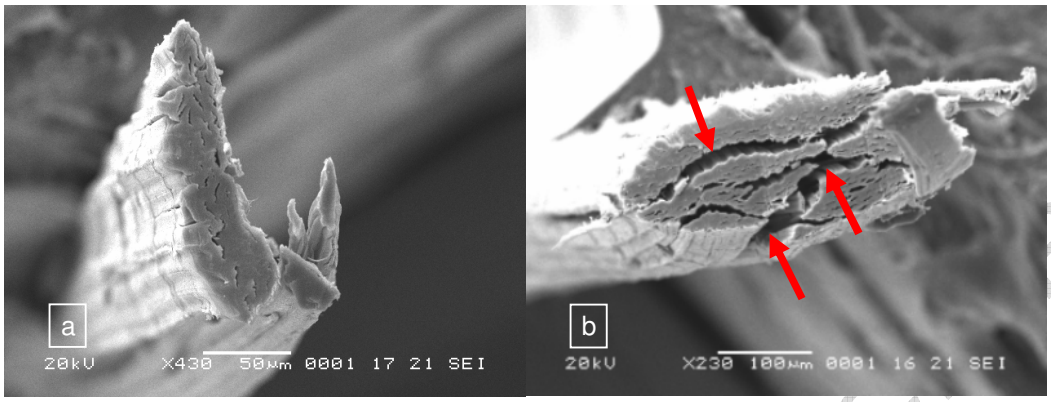

Cross-sectional area for a single abaca fibre bundle before (a) and after (b) tensile testing. The arrows indicate cracks.

Figure 4

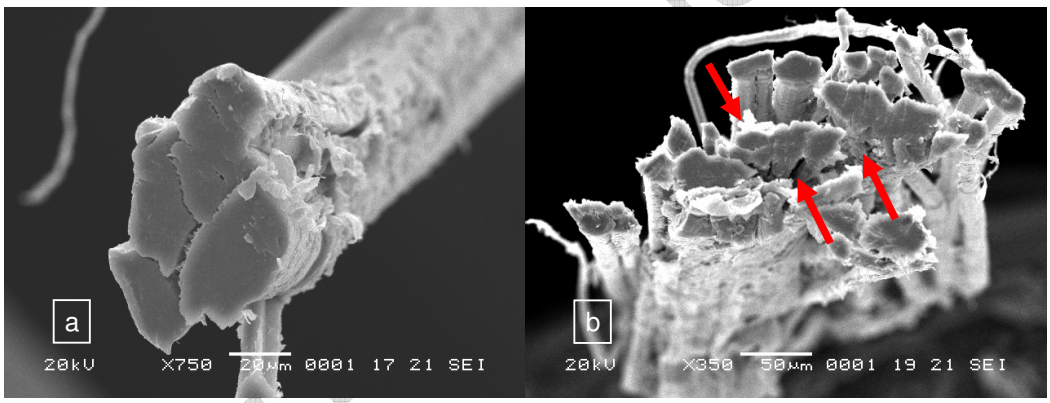

Cross-sectional area for a single flax fibre bundle before (a) and after (b) tensile testing. The arrows indicate cracks.

Figure 5

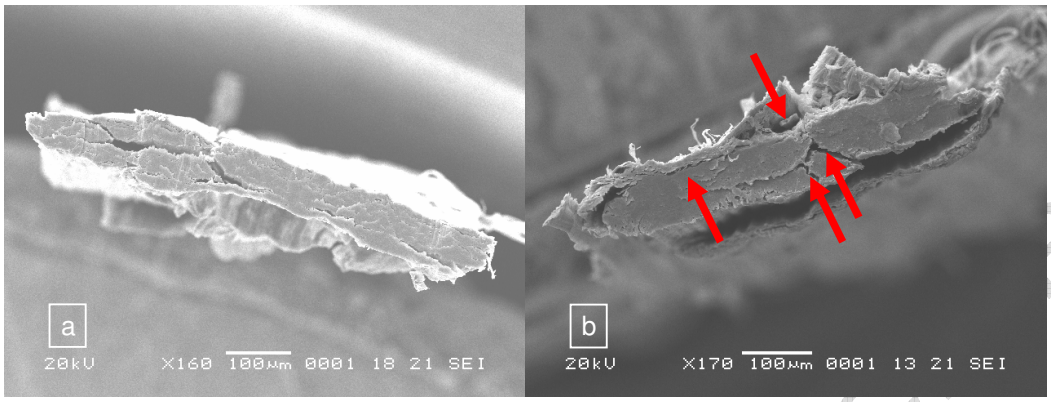

Cross-sectional area for a single hemp fibre bundle before (a) and after (b) tensile testing. The arrows indicate cracks.

Figure 6

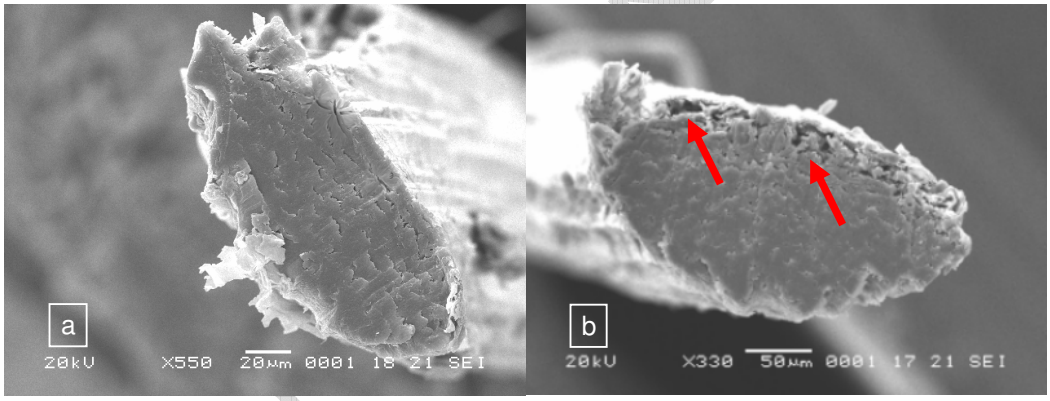

Cross-sectional area for a single sisal fibre bundle before (a) and after (b) tensile testing. The arrows indicate cracks.

Figure 7

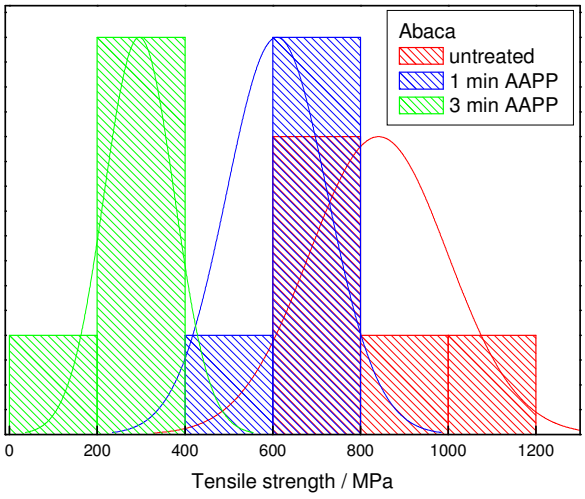

Figure 8a

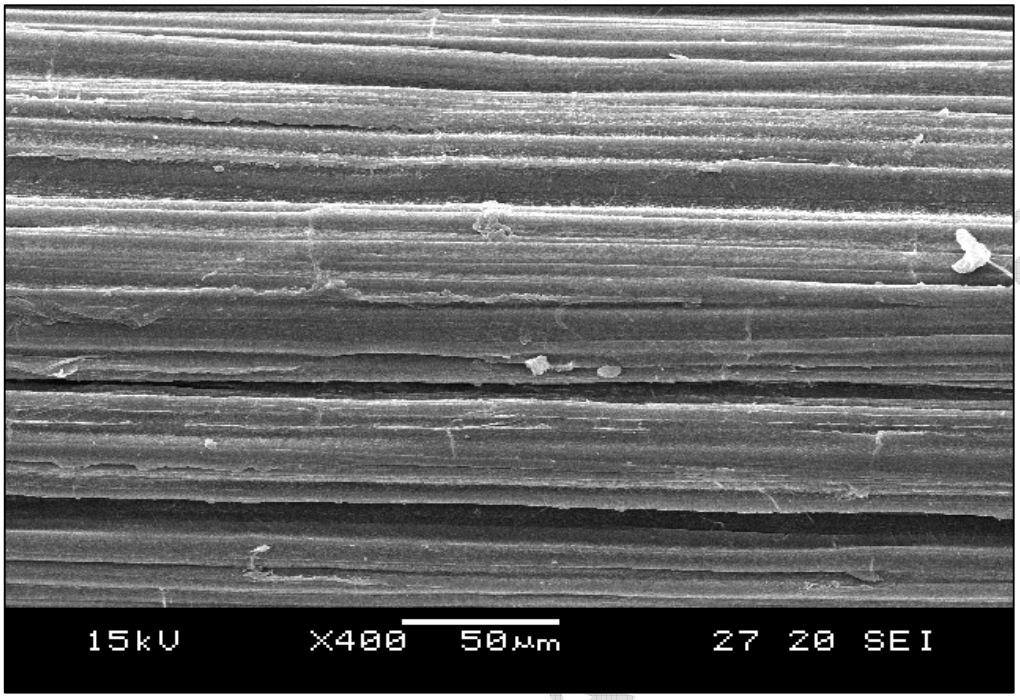

Surface morphology for an untreated single abaca fibre bundle.

Figure 8b

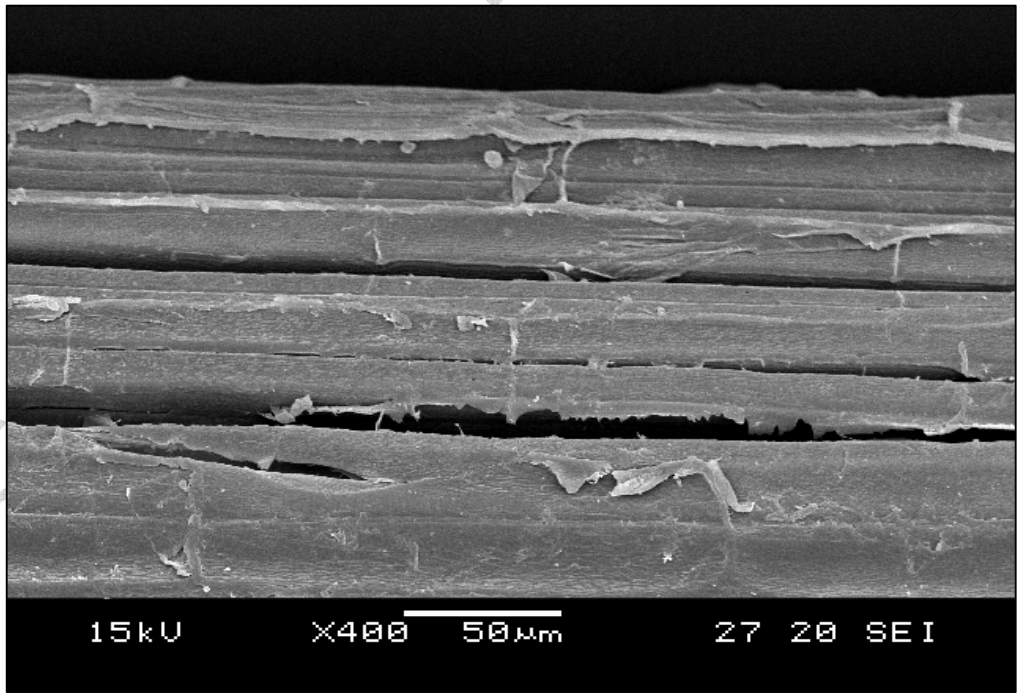

Surface morphology for a 1 min AAPP-treated abaca fibre bundle.

Figure 8c

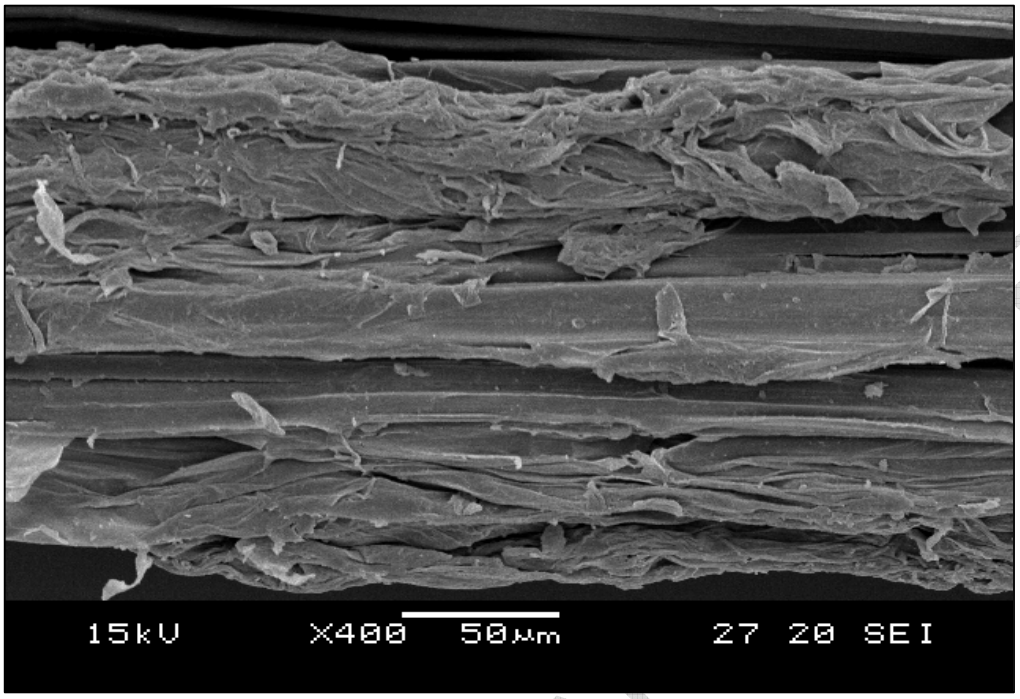

Surface morphology for a 3 min AAPP-treated abaca fibre bundle.

Figure 9a

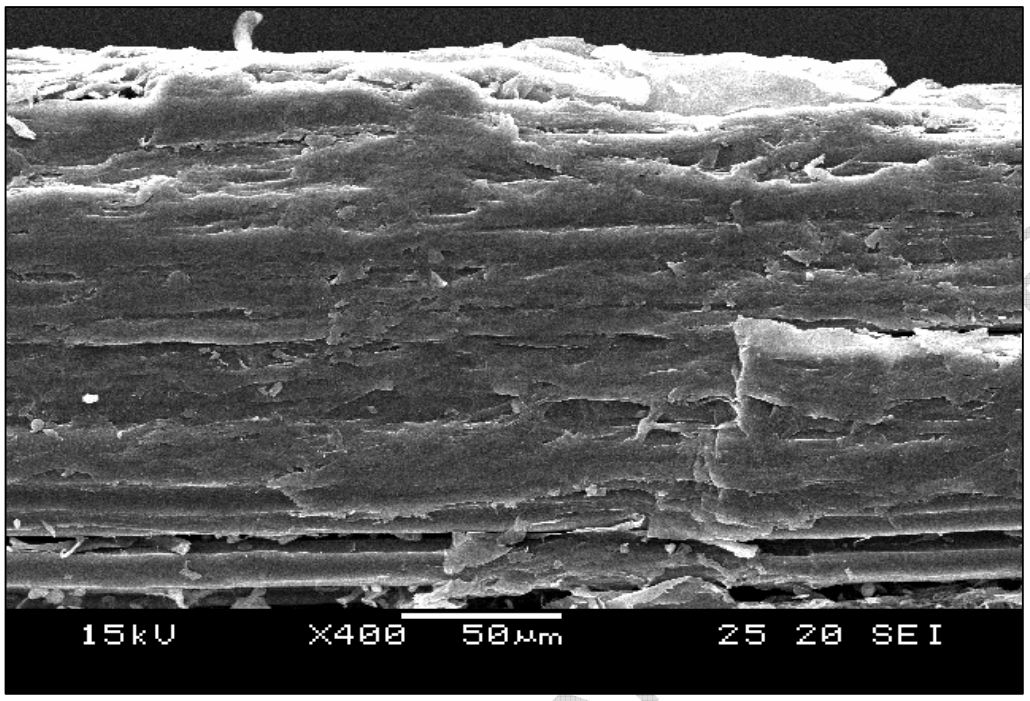

Surface morphology for an untreated single flax fibre bundle.

Figure 9b

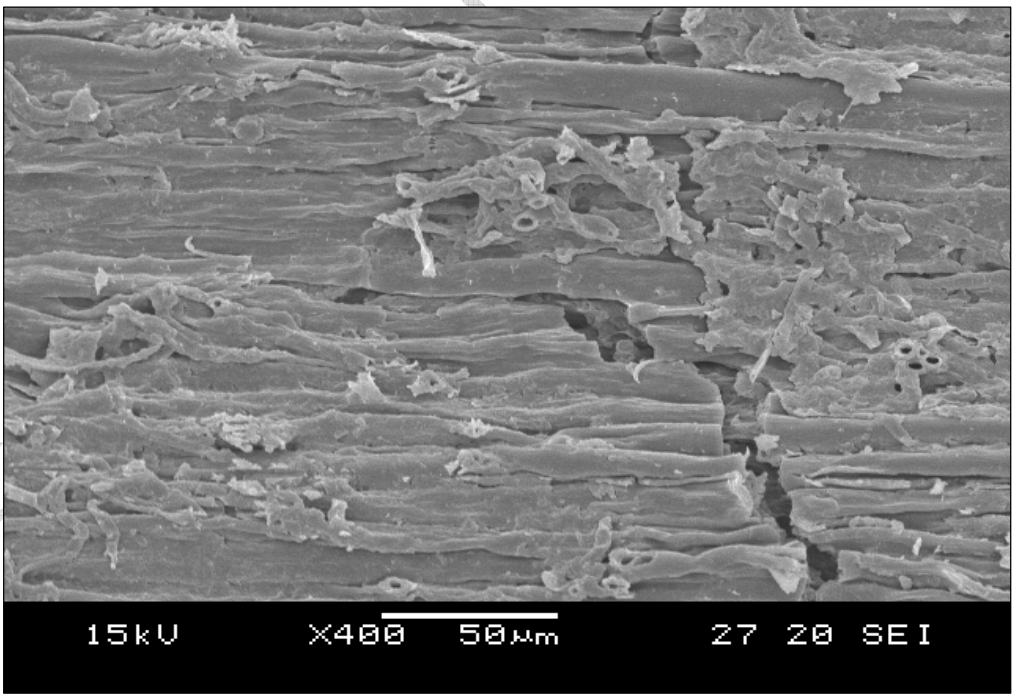

Surface morphology for a 1 min AAPP-treated flax fibre bundle.

Figure 9c

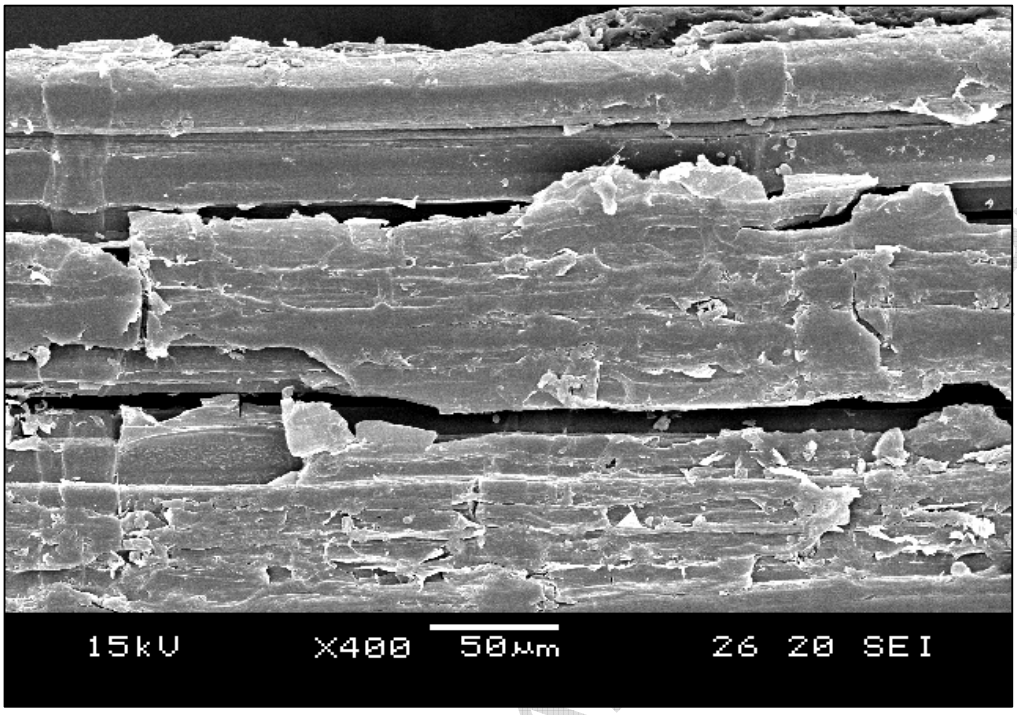

Surface morphology for a 3 min AAPP-treated flax fibre bundle.

Figure 10a

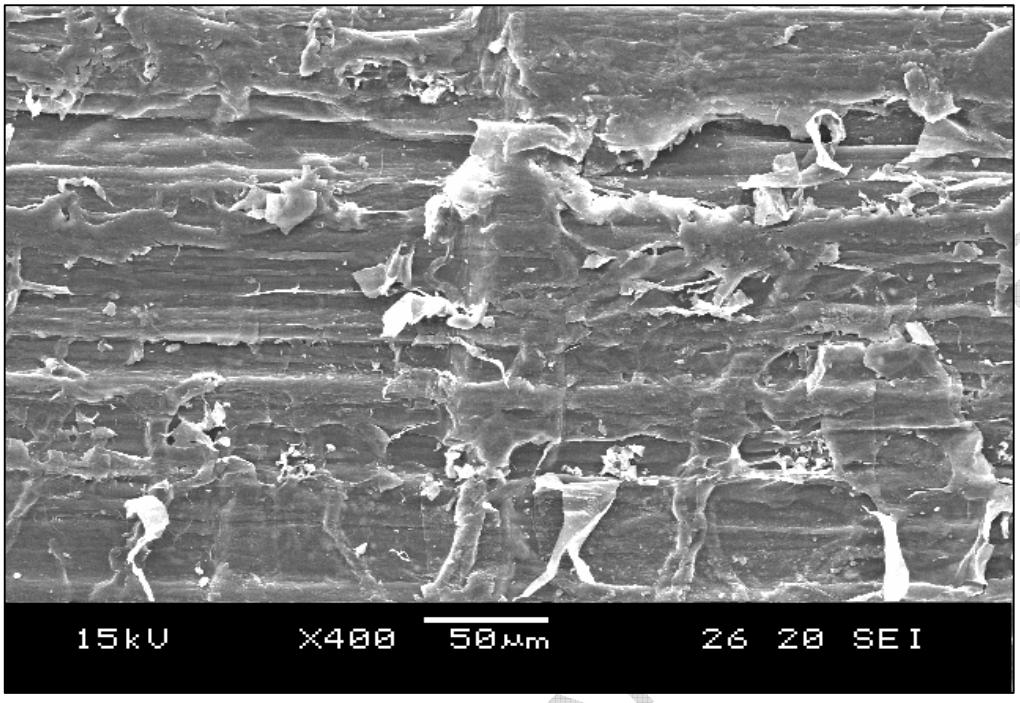

Surface morphology for an untreated single hemp fibre bundle.

Figure 10b

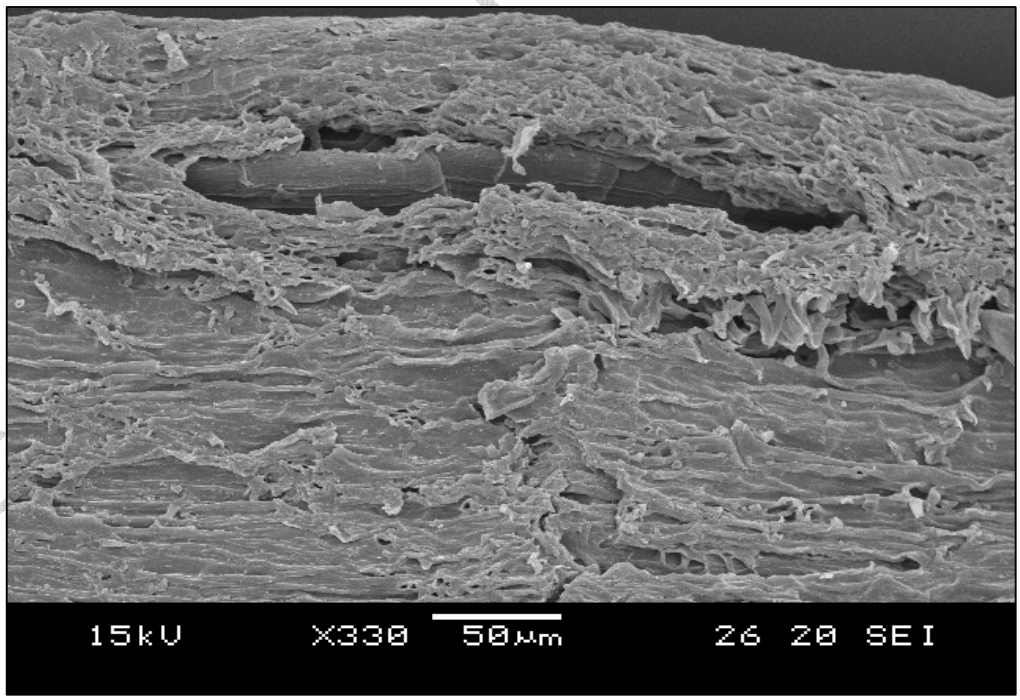

Surface morphology for a 1 min AAPP-treated hemp fibre bundle.

Figure 10c

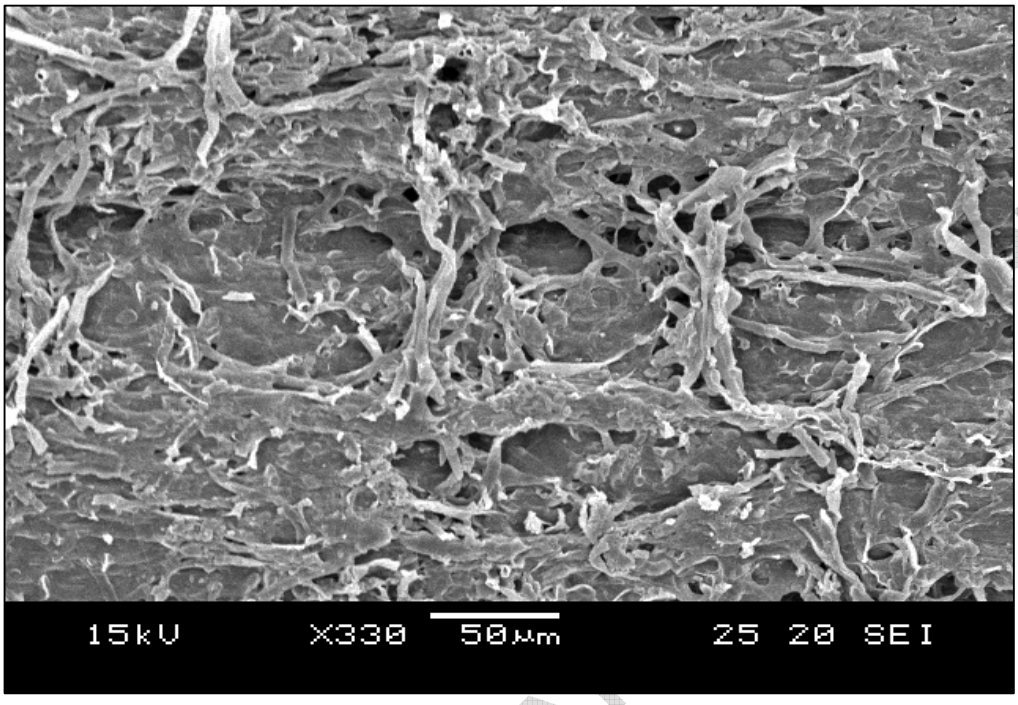

Surface morphology for a 3 min AAPP-treated hemp fibre bundle.

Figure 11a

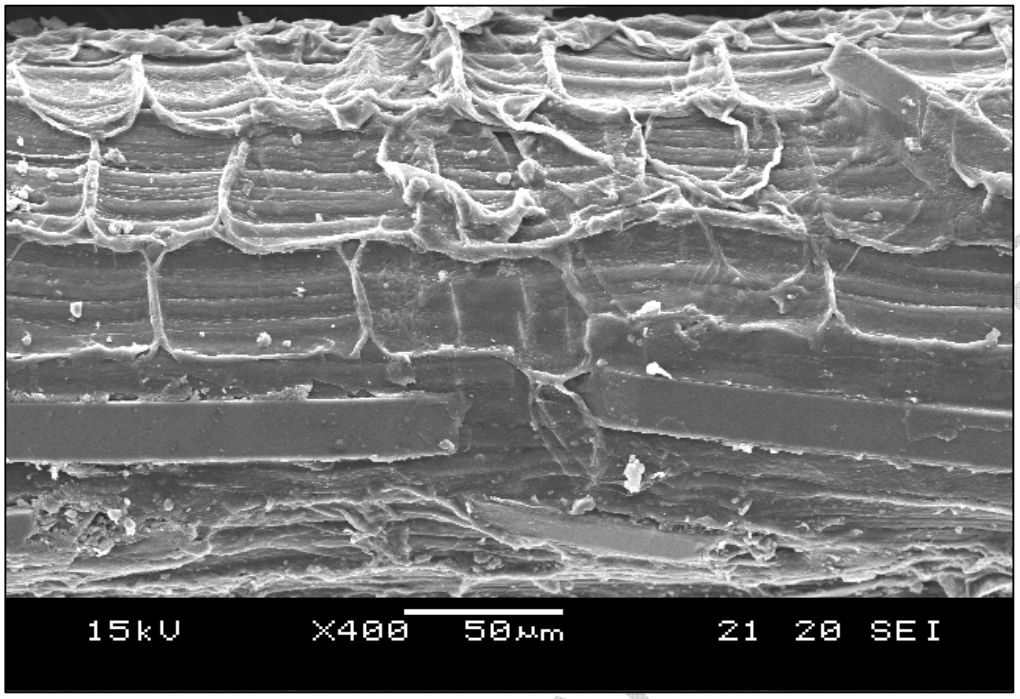

Surface morphology for an untreated single sisal fibre bundle.

Figure 11b

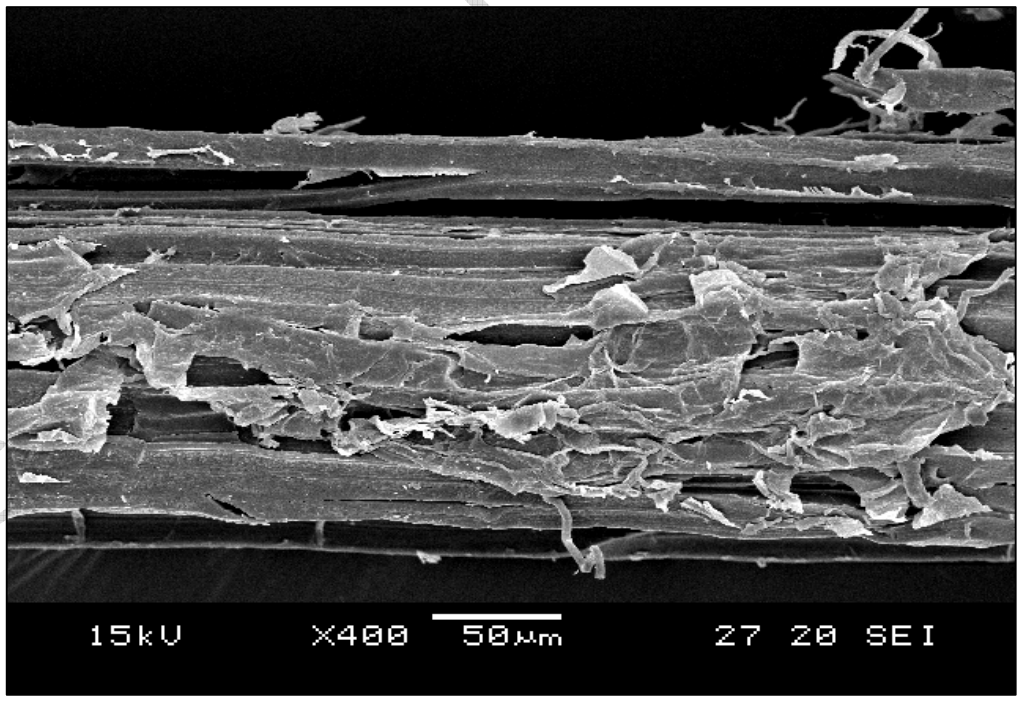

Surface morphology for a 1 min AAPP-treated sisal fibre bundle.

Figure 11c

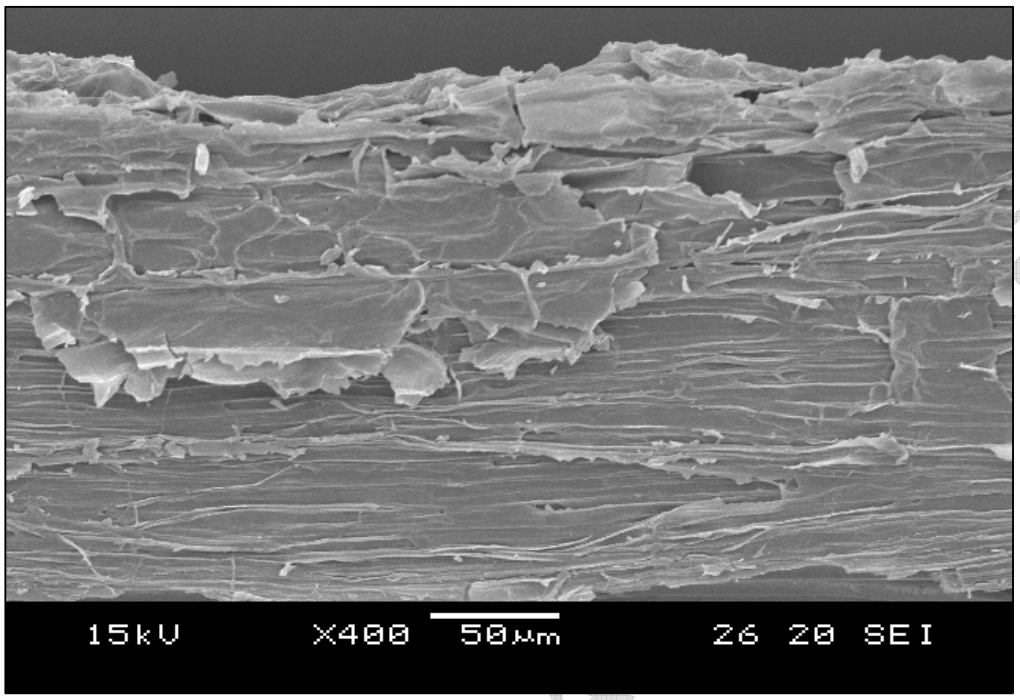

Surface morphology for a 3 min AAPP-treated sisal fibre bundle.

Figure 13

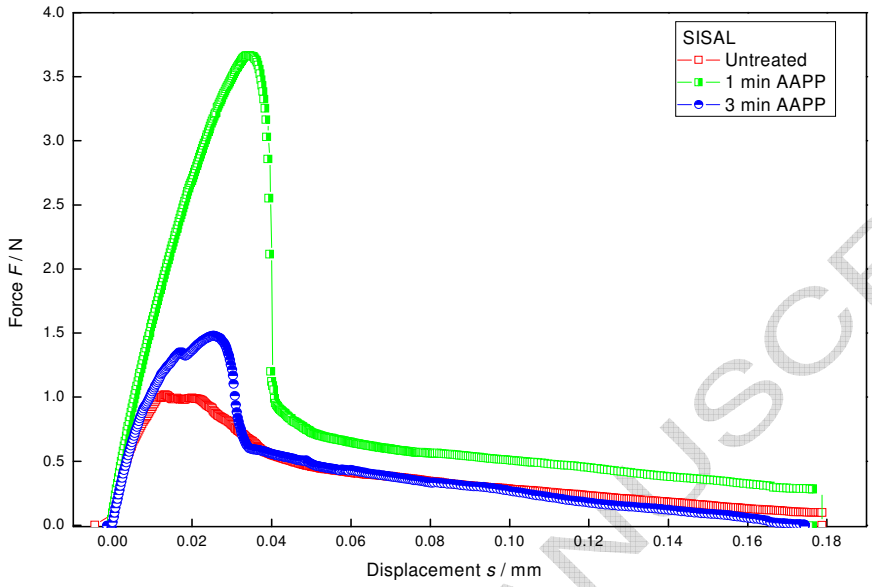

Fig. 14a

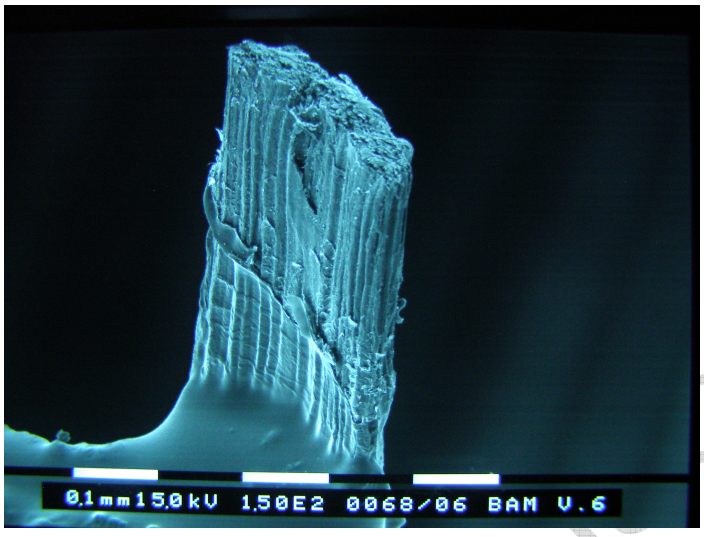

Fig. 14b

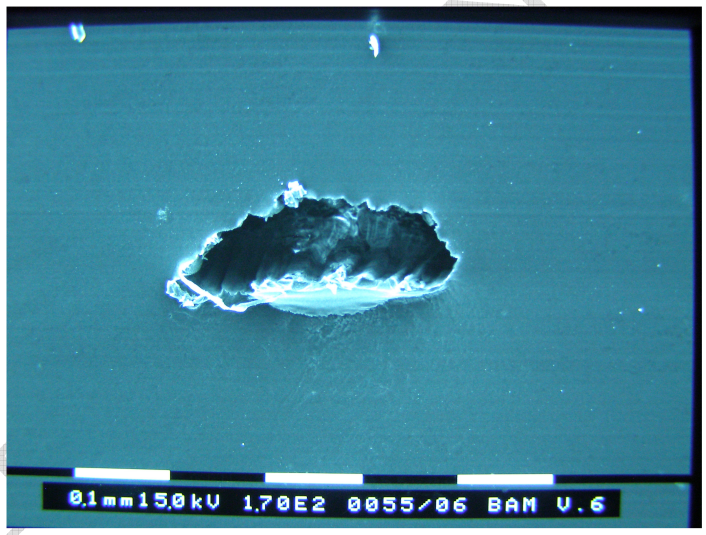

Fig. 14c

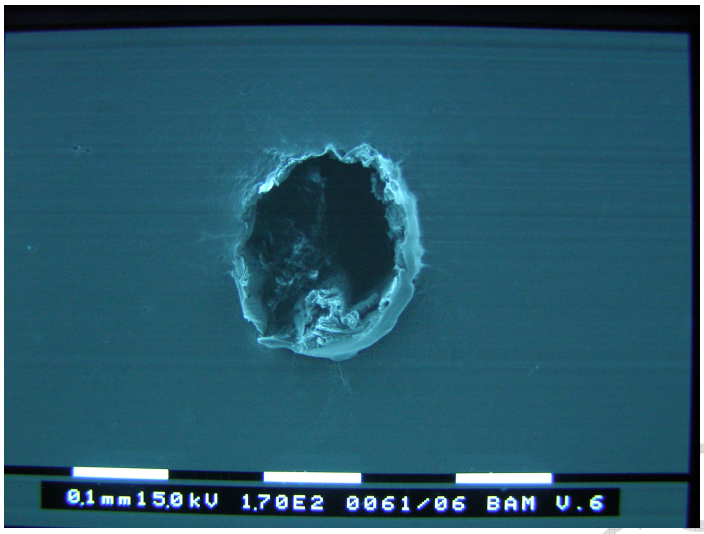

1
2

Figure 15

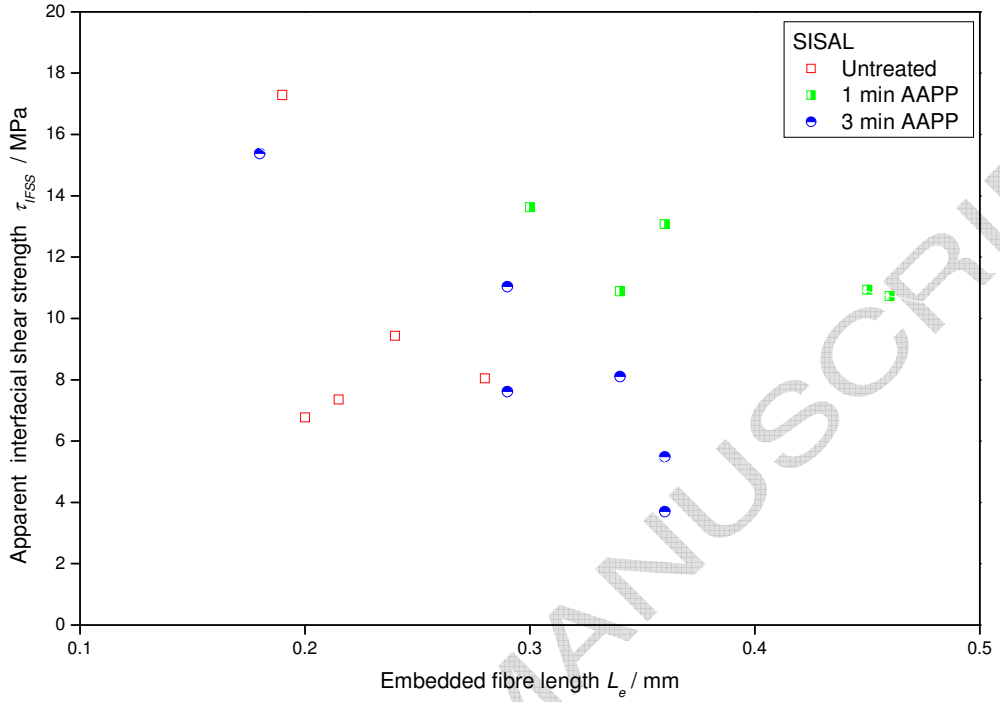

Figure 16

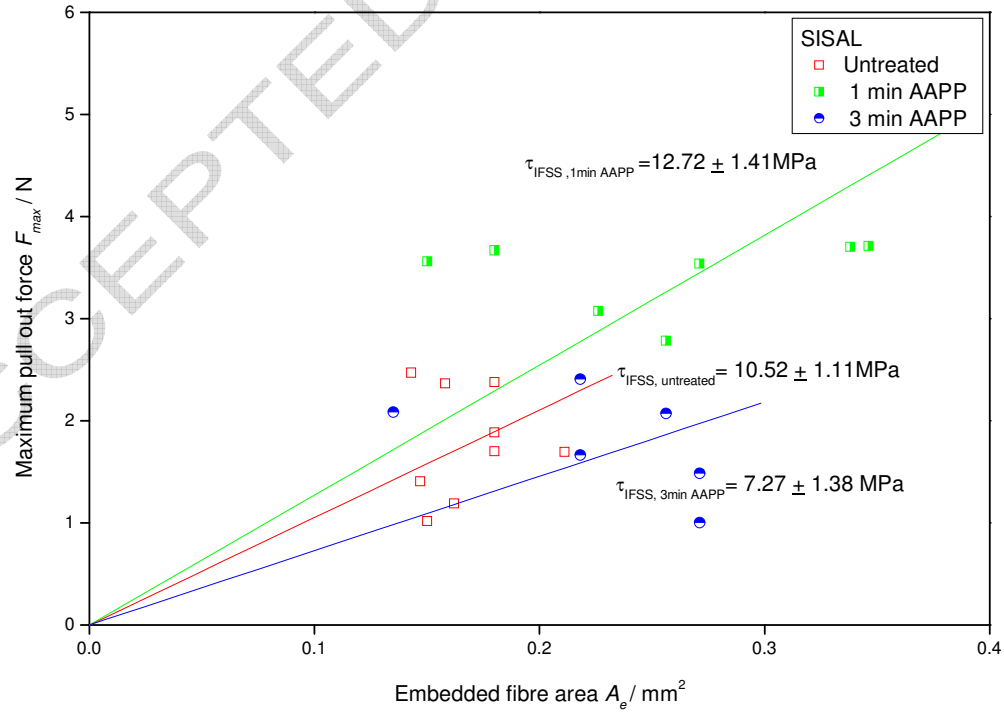

CAPTIONS

TABLES

Table 1

Fibre	Cellulose (wt.-%)	Lignin (wt.-%)	Hemicelluloses (wt.-%)	Ash Content (wt.-%)
Abaca	63.7	15.1	17.5	1.1
Flax	75.2	4.8	8.6	1.1
Hemp	75.1	8	< 2.0	3.5
Sisal	47.6	10.6	17.8	4.5

Table 2

		Untreated			1 min AAPP			3 min AAPP		
Abaca	**Diameter (µm)**	**Tensile strength (Mpa)**	**Young's modulus (GPa)**	**Elongation at break (%)**	**Tensile strength (Mpa)**	**Young's modulus (GPa)**	**Elongation at break (%)**	**Tensile strength (Mpa)**	**Young's modulus (GPa)**	**Elongation at break (%)**
Abaca										
5	179 ± 47	873.4 ± 167.7	12.3 ± 2.5	10 ± 1.1	604.3 ± 225.4	9 ± 2.2	6.8 ± 1.4	490.3 ± 150.7	11 ± 3.4	6 ± 1.9
10		798.5 ± 145.7	18.4 ± 2.9	6.2 ± 1.2	574.7 ± 123.5	14.5 ± 3	4.4 ± 0.7	302.7 ± 59.9	10.1 ± 1.9	4 ± 0.7
20		911 ± 224.8	25.4 ± 0.7	4.5 ± 0.9	585.8 ± 78	22.6 ± 2.1	3 ± 0.6	352.1 ± 138.8	15.4 ± 6	2.8 ± 0.6
50		918.7 ± 214.6	30 ± 5.1	3.9 ± 0.5	494.9 ± 207.6	23.3 ± 7.5	2.5 ± 0.5	335.9 ± 87.5	21.5 ± 4	2 ± 0.5
Flax										
5	130 + 27	1374.3 ± 337.2	19.4 ± 3.7	7.9 ± 1.6	1141.2 ± 395.3	17.4 ± 6.1	6.4 ± 1.9	876.5 ± 390.6	11.9 ± 3.9	5.5 ± 2.1
10		1277.3 ± 590.7	48 ± 16	4.7 ± 1.6	1155.2 ± 441.5	23.7 ± 5.7	3.6 ± 0.8	1002.6 ± 540.8	19.2 ± 8.6	3.3 ± 1.3
20		1272.1 ± 377	75 ± 12.9	3.3 ± 0.6	406 ± 116.9	25 ± 8	3 ± 1.4	377 ± 314	17.8 ± 6.7	2.6 ± 0.7
50		1755.7 ± 304	130.1 ± 22.4	2.3 ± 0.5	393 ± 226	30.9 ± 16.6	1.9 ± 0.6	340 ± 207.9	17.1 ± 4.9	1.4 ± 0.5
Hemp										
5	205+ 65	1125.5 ± 400.8	17 ± 6.1	9 ± 3.2	705.4 ± 350.5	15.3 ± 5.5	5.6 ± 2.1	498 ± 233	12.2 ± 3.8	5 ± 1.9
10		1178 ± 231.7	68.5 ± 23.5	6.4 ± 0.9	448.5 ± 231.6	19.4 ± 7.8	3.6 ± 1.6	377 ± 115	16.8 ± 9.8	3.1 ± 0.8
20		604.9 ± 315.2	40.4 ± 21	3.7 ± 0.6	197.2 ± 36.9	15.1 ± 3.2	2.4 ± 1	184 ± 87	11.4 ± 6.4	1.9 ± 0.8
50		1078.4 ± 435.6	51.7 ± 14.7	3.1 ± 0.4	191.1 ± 82.9	24.2 ± 9.2	2.3 ± 1.8	161 ± 79	15.4 ± 5	1.2 ± 0.7
Sisal										
5	310 + 66	1483 ± 371.2	19 ± 1.9	12.8 ± 3.5	1146.3 ± 541.7	18.3 ± 7.3	6.8 ± 2.1	953.2 ± 323.8	11.3 ± 1.7	5.2 ± 1.4
10		1556.8 ± 73.3	32.2 ± 7.3	6.6 ± 1.5	955.2 ± 329.2	26.7 ± 8.7	4.2 ± 0.8	875 ± 94.8	14.6 ± 2.9	3.9 ± 1.3
20		1577.6 ± 422.7	35.1 ± 10.9	6.3 ± 1.5	1042.1 ± 95.1	33 ± 3.6	4.4 ± 1.7	531.1 ± 234.5	13.8 ± 4.8	3.5 ± 0.8
50		1358.3 ± 449.2	40.1 ± 19	5.1 ± 1.6	1015.5 ± 456.4	37.9 ± 14.7	2.9 ± 0.5	755.9 ± 231.5	20.9 ± 4.1	1.9 ± 0.7

Table 3

		W-statistic			P-statistic		
Fibre		**Original**	**1 min AAPP**	**3 min AAPP**	**Original**	**1 min AAPP**	**3 min AAPP**
Abaca	5	0.95920	0.89664	0.94886	0.80355	0.13725	0.63924
	10	0.89262	0.88284	0.94382	0.3678	0.1341	0.57987
	20	0.94515	0.94173	0.88641	0.71015	0.5559	0.14725
	50	0.85011	0.90897	0.97780	0.19161	0.26187	0.94729
Flax	5	0.88426	0.96118	0.87550	0.32648	0.76678	0.11057
	10	0.93623	0.92059	0.92061	0.64671	0.34736	0.30879
	20	0.96049	0.91265	0.96862	0.81154	0.25018	0.85714
	50	0.97128	0.92042	0.94036	0.87462	0.34595	0.54049
Hemp	5	0.95694	0.92323	0.93695	0.78925	0.36972	0.46463
	10	0.83917	0.95238	0.92553	0.11942	0.65231	0.3505
	20	0.89360	0.92895	0.95128	0.33162	0.56051	0.63807
	50	0.94927	0.90857	0.92732	0.68209	0.30102	0.36687
Sisal	5	0.97202	0.91014	0.87688	0.8787	0.23382	0.0522
	10	0.86231	0.95227	0.94777	0.23347	0.68024	0.59316
	20	0.95368	0.92313	0.91641	0.76816	0.46065	0.31428
	50	0.98735	0.93495	0.96745	0.95793	0.48186	0.85642

Table 4

	τ_{IFSS} (MPa)		
Fibre	**Untreated**	**1 min AAPP**	**3 min AAPP**
Abaca	16.85 $\pm$ 1.45	10.17 $\pm$ 1.45	9.77 $\pm$ 0.29
Flax	8.12 $\pm$ 0.50	9.36 $\pm$ 1.58	-
Hemp	8.44 $\pm$ 1.84	9.44 $\pm$ 1.31	-
Sisal	10.52 $\pm$ 1.11	12.72 $\pm$ 1.41	7.27 $\pm$ 1.38

1 Table 5

Fibre	Untreated	1 min AAPP	3 min AAPP
Abaca			
L_c (mm)	18	22	12
σ (MPa)	799	575	303
d (mm)	0.779	0.779	0.779
τ_{FSS} (MPa)	16.85	10.17	9.77
Flax			
L_c (mm)	55	43	-
σ (MPa)	1277	1155	1003
d (mm)	0.701	0.701	0.701
τ_{FSS} (MPa)	8.12	9.36	-
Hemp			
L_c (mm)	137	18	-
σ (MPa)	3009	448	377
d (mm)	0.768	0.768	0.768
τ_{FSS} (MPa)	8.44	9.44	-
Sisal			
L_c (mm)	56	28	45
σ (MPa)	1577	955	875
d (mm)	0.752	0.752	0.752
τ_{FSS} (MPa)	10.52	12.72	7.27

2